Hindawi Publishing Corporation
Mathematical Problems in Engineering
Volume 2013, Article ID 562410, 7 pages
http://dx.doi.org/10.1155/2013/562410

Research Article

An Elastoplastic Damage Constitutive Model for Cementitious Materials under Wet-Dry Cyclic Sulfate Attack

Da Chen, Chen Du, Xingguo Feng, and Feng Ouyang

College of Harbour, Coastal, and Offshore Engineering, Hohai University, Nanjing 210098, China

Correspondence should be addressed to Feng Ouyang; decolor@163.com

Received 7 February 2013; Revised 17 April 2013; Accepted 22 April 2013

Academic Editor: Irene Penesis

The mechanical properties of cement mortars subjected to wet-dry cyclic sulfate attack were studied by the compression strength test. The results showed that the ultimate compressive strength increased with number of cycles at the initial stage. However, after a certain time, it started to decrease with further increases in the number of cycles. Moreover, the concentration of the sodium sulfate solution proved to be an important factor affecting the ultimate compressive strength. Based on continuum damage mechanics theory, an elastoplastic damage constitutive model is presented to describe the mechanical behavior of cementitious materials under compressive stress. The results obtained agree well with the experimentally observed elastic, plastic, and damage characteristics of cement mortars under compressive stress.

1. Introduction

Sulfate attack is one of the most aggressive forms of environmental deterioration affecting the long-term durability of concrete structures [1]. As concrete suffers sulfate attack, the sulfate ions react with calcium hydroxide and calcium aluminate hydrate and form more voluminous phases [2] (gypsum and ettringite). The formation of gypsum and ettringite leads to expansion, cracking, deterioration, and disruption of concrete structures. Studying the mechanical and mineralogical properties of cement mortar with different pozzolanic compositions in a sulfate medium, Ahmet and Sükrü [1] concluded that compact structures have more effective properties against sulfate attack. In addition, these results indicated that the formation of gypsum causes cracks inside the mortar, and the formation of ettringite causes spalling on the surface of mortar. Irassar et al. [3] used X-ray diffraction to study mortar specimens (containing limestone filler) exposed for two years to sodium sulfate solution and found that the sulfate attack is characterized by an inward movement of the reaction. The first reaction in mortar was the formation of ettringite; later, gypsum deposition occurred, followed by thaumasite formation. Lee et al. [4] studied the effectiveness of silica fumes in controlling the damage arising from sulfate attack. The results showed that the presence of silica fumes had a beneficial effect on strength for mortars exposed to a sodium sulfate environment. However, mortars containing silica fumes were severely damaged in a magnesium sulfate environment. In addition, the compressive strength results indicated that the water-to-cementitious materials ratio is the most critical parameter influencing the resistance of concrete to sulfate attack. Investigating the effect of sulfate attack on the dynamic strength and deformation characteristics of concrete using the compression test, Liu et al. [5] reported that the compressive strength, elastic modulus, peak strain, and energy absorption capacity of concrete suffering from sulfate attack tend to decrease compared with control samples (concrete cured in a room environment without sulfate attack). Assuming the sulfate attack process to be a function of time incorporating diffusion, chemical reaction, and structural damage, Sarkar et al. [6] proposed a continuum damage mechanics model to assess the degradation of cementitious materials under sulfate attack and reported that the model could be used to determine ion and mineral profiles. Idiart et al. [7] presented a chemomechanical model to assess the degradation of concrete subjected to external sulfate attack. The results showed that the coupling effect (effect of cracks on the reactive transport process) is very important in the case

of external sulfate attack. Cracks represent preferential penetration channels for the diffusion of sulfates into the sample. In turn, the acceleration of the diffusion-reaction process leads to a higher degree of mechanical degradation.

Concrete structures exposed to marine environments have always suffered from sulfate attack. In particular, the deterioration of concrete members placed in the tidal zone is more pronounced because of wet-dry cycles. To simulate sulfate attack on offshore concrete structures, a wet-dry cyclic sulfate attack process was examined here. The evolution of the mechanical properties of mortars suffering wet-dry cyclic sodium sulfate attack was studied. In addition, an elastoplastic damage model was proposed to describe the mechanical behavior of these mortars under compression. The constitutive model presented here could be used to assess the degradation of the mechanical properties of concrete exposed to wet-dry sulfate attack. For example, it could be used to estimate the degradation of concrete structures exposed to the tidal zone in offshore engineering.

2. Experiments

2.1. Materials and Experiments. Cubic samples, of size 70.7 mm and prepared with ordinary Portland cement (P.O 42.5), were used in this study. The sand-cementitious material ratio and the water-cement ratio (W/C) of the mortars were kept at 3 and 0.5, respectively. The mortar samples were removed from their molds after 24 h. Cement mortar samples were maintained for 28 days in a curing chamber, where the temperature and humidity were kept at $20 \pm 2^{\circ}$C and $95 \pm 3\%$, respectively. After this, the samples were dried in a drying oven at $80 \pm 5^{\circ}$C for 48 h. The dried specimens were then prepared for the wet-dry cyclic sulfate attack experiment. For each cycle, after 16 h immersed in Na_2SO_4 solution, the samples were dried in air for 1 h. Then, the samples were dried at $80 \pm 5^{\circ}$C for 6 h and cooled at room temperature for 1 h. Afterwards, the samples were reimmersed in the sulfate solution and started a new wet-dry cycle. Solutions containing 0.5%, 5%, and 10% sodium sulfate were chosen for the wet-dry cycle tests. After different wet-dry cycle times, compression tests were conducted with a universal testing machine at a rate of 0.02 mm/min.

2.2. Results. According to the results shown in Figure 1, the stress-strain curves of the mortars started with a linear rampup but then showed loss of linearity. Liu et al. [5] had reported the nonlinear zone (before reaching ultimate strength) and attributed it to the formation of interior cracks in the mortars. After reaching peak stress, the compressive stress decreased rapidly, and visible cracks formed. As the strain further increased, the mortar fractured.

As shown by the results for ultimate compressive strength (Figure 2), the strength increased with number of cycles in the early stages. However, after a certain time, it began to decrease with further increases in the number of cycles. Moreover, the transition time to ultimate compressive strength decreased with increasing sulfate concentration. For example, for mortars exposed to 0.5% sodium sulfate solution, the transition occurred after 90 wet-dry cycles. However, the transition occurred after only 60 cycles for mortars exposed to 10% sodium sulfate solution. Moreover, variations in compression strength were more significant for the samples exposed to the higher concentration sulfate solution.

3. Numerical Modeling of Sulfate Attack

3.1. Mechanical Damage. In the present study, an elastoplastic damage model is proposed. For simplicity in applying the model in the engineering domain, the damage state of materials is assumed to be isotropic. The bulk modulus k and the shear modulus μ can fully characterize the elastic behavior of isotropic materials. Cementitious materials in structures suffer mainly from compressive stress. Under compressive stress, the failure mechanism of materials presents mainly in the form of shear failure. Compared with the variance in shear modulus, the change of bulk modulus under compressive stress is small. Therefore, similar to Lemaitre's model [8], it is assumed here that only the parameter μ is affected by material damage. The effect of the mechanical damage variable d_1 on μ can be expressed as follows:

$$\mu(d_1) = \mu_0(1 - d_1), \tag{1}$$

where μ_0 is the shear modulus of undamaged materials. As a result, the thermodynamic potential of a damaged material can be expressed as

$$\psi^e(\varepsilon^e, d_1) = \frac{1}{2}\left[k(\varepsilon_v^e)^2 + 2\mu(d_1)\, e_{ij}^e e_{ij}^e\right], \tag{2}$$

where ε_v^e is the elastic volumetric strain and e_{ij}^e is the components of an elastic deviation strain tensor. Therefore, the stress-strain relation of the damaged material can be expressed as follows:

$$\sigma_{ij} = \frac{\partial \psi^e}{\partial \varepsilon^e} = k\,\mathrm{tr}(\varepsilon^e)\,\delta_{ij} + 2\mu(d_1)\, e_{ij}^e = C(d_1) : \varepsilon^e, \tag{3}$$

where $C(d_1)$ is the effective stiffness tensor. Consequently, the stress increment can be expressed as

$$d\sigma = C(d_1) : d\varepsilon^e + \dot{C}(d_1) : \varepsilon^e d(d_1). \tag{4}$$

In addition, the conjugate force (Y_d) associated with the damage variable is defined by

$$Y_d = -\frac{\partial \psi^e}{\partial d_1} = \mu_0 e_{ij}^e e_{ij}^e. \tag{5}$$

Note that the theory expressed above is based on the assumption that the materials maintain an elastic state. In fact, plastic deformation occurs in mortar during the compressive process. Therefore, a heuristic approach has been proposed to express the effect of plastic strain on damage evolution. Moreover, damage evolution was thought to depend separately on elastic and plastic strains. To express this relationship, the driving force (ξ_d) was introduced to explain damage evolution and can be defined as follows:

$$\xi_d = \mu_0\left(e_{ij}^e e_{ij}^e + e_{ij}^p e_{ij}^p\right), \tag{6}$$

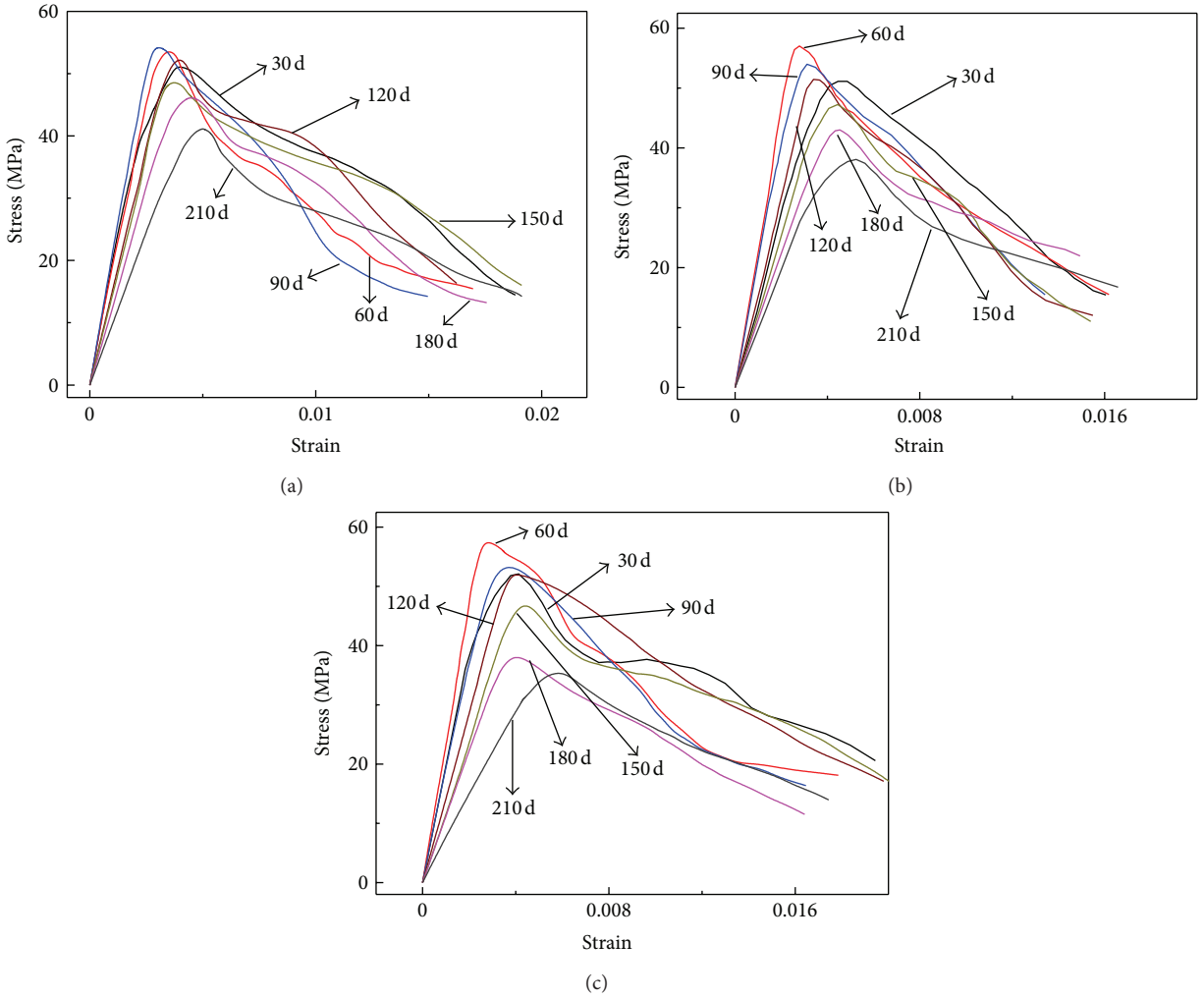

FIGURE 1: Compressive stress-strain curves of samples experiencing different numbers of wet-dry cycles: (a) in 0.5% sodium sulfate solution; (b) in 5% sodium sulfate solution; (c) in 10% sodium sulfate solution.

where e_{ij}^{p} is the components of the plastic deviation strain tensor. Including the plastic deformation effects, the stress increment can be expressed as follows:

$$d\sigma = C(d_1) : (d\varepsilon - d\varepsilon^{p}) + \dot{C}(d_1) : (\varepsilon - \varepsilon^{p})\, d(d_1). \quad (7)$$

To assess the mechanism of material damage, an exponential function [9] was introduced to describe damage evolution:

$$f_d = A_1 - \frac{A_1}{\exp\left[B\left(\xi_d - \xi_d^0\right)\right]} - d_1 = 0. \quad (8)$$

The parameter A_1 defines a critical value of damage corresponding to the residual strength of damaged material. B controls the kinetics of damage evolution, and ξ_d^0 defines the threshold of damage force. Therefore, the mechanical damage variable d_1 can be expressed as follows:

$$d_1 = A_1 - \frac{A_1}{\exp\left[B\left(\xi_d - \xi_d^0\right)\right]}. \quad (9)$$

3.2. Chemical Damage. Under sulfate attack, ettringite and gypsum minerals form in mortar [1]. As the formed sulfate minerals exceed a certain amount, they can cause partial breakage of the mortar. Furthermore, the breakage can be defined by the degradation of compressive strength:

$$d_2 = A_2 - A_2 \frac{f_c}{f_{c0}}, \quad (10)$$

where d_2 is the chemical damage variable, f_{c0} and f_c are the ultimate compressive strengths of the undamaged samples, and the sulfate-attacked samples respectively, and A_2 defines a critical value of damage corresponding to the residual strength of the chemically damaged material.

The compressive strengths of the samples are closely related to the concentration of the sulfate solution (c) and the number of wet-dry cycles (t). Therefore, the compressive strength can be expressed as follows:

$$f_c = f_{c0}\, f(c, t), \quad (11)$$

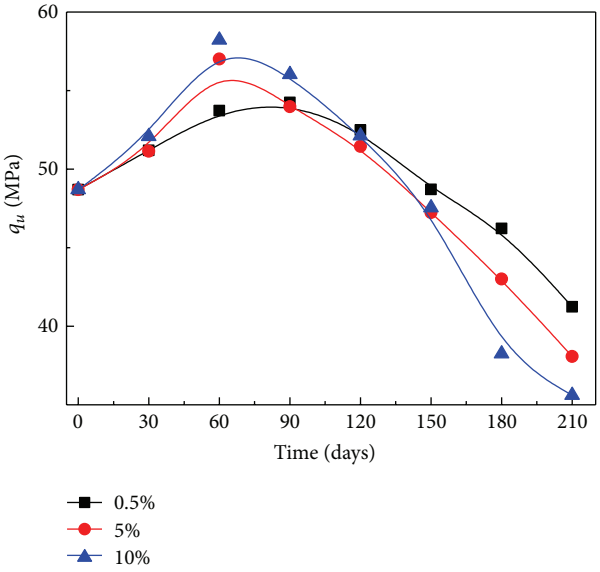

FIGURE 2: Ultimate strength of samples experiencing different numbers of wet-dry cycles.

where $f(c,t)$ is a function of the sulfate concentration (c) and the number of wet-dry cycles (t). Then, combining (10) and (11), the following expression for d_2 can be written:

$$d_2 = A_2 - A_2 f(c,t). \tag{12}$$

Xu [10] has reported that there is a power function relationship between compressive strength and sulfate attack time. In addition, a linear relationship between compressive strength and sulfate concentration has also been determined. Based on experimental data, compressive strength can be expressed as a function of sulfate concentration and sulfate attack time as follows:

$$\begin{aligned} f(c,t) = {} & (-0.0362c - 1.2107)\, t^{1.25} \times 10^{-3} \\ & + (0.3876c + 47.342)\, t^{0.25} \times 10^{-2}. \end{aligned} \tag{13}$$

It has been assumed in this study that chemical damage to materials can be described by thermodynamic theory. The scalar damage variable (D) can be physically identified as a microcrack density [9]. For concrete materials suffering from sulfate attack (chemical damage), the formed gypsum and ettringite lead to the formation of internal cracks in the concrete. Therefore, the mechanical properties of concrete are affected by chemical damage. In fact, the intrinsic characteristics of chemical damage are the same as those of mechanical damage. Both mechanical and chemical damage appear incrementally during the damages process. Therefore, the total damage (D) to materials, which includes mechanical damage (d_1) and chemical damage (d_2), can be expressed as follows:

$$D = d_1 + d_2 = A_1 \left\{ 1 - \frac{1}{\exp\left[B\left(\xi_d - \xi_d^0\right)\right]} \right\} + A_2 \left(1 - \frac{f_c}{f_{c0}} \right). \tag{14}$$

3.3. Plasticity Characteristics. Small strains and isothermal conditions were assumed in the present study. The total strain tensor is composed of an elastic part and a plastic part as follows:

$$d\varepsilon_{ij} = d\varepsilon_{ij}^e + d\varepsilon_{ij}^p. \tag{15}$$

During the microcrack extension process, local plastic deformation of mortar induced stress redistribution. To account for this redistribution of stresses, an effective stress tensor $\widetilde{\sigma_{ij}}$ for damaged material has been introduced and is defined as follows [10]:

$$\widetilde{\sigma_{ij}} = \sigma_m \delta_{ij} + \frac{S_{ij}}{1 - D}, \tag{16}$$

$$\sigma_{ij} = \sigma_m \delta_{ij} + S_{ij}, \tag{17}$$

where D is the total damage to materials and σ_m and S_{ij} represent the nominal mean stress and the components of the nominal deviation stress tensor, respectively. Compared with the classical model used in continuum damage mechanics [10], the proposed model presented in (16) is a more general form.

The classic Mohr-Coulomb criterion [11] based on linear rules was used in the present study to describe the failure surface of the mortar:

$$F = c_1 \frac{\widetilde{\sigma_{\mathrm{eq}}}}{f_{c0}} - c_2 - \frac{\widetilde{I}}{f_{c0}} = 0, \tag{18}$$

where $\widetilde{I}$ is the mean stress, $\widetilde{\sigma_{\mathrm{eq}}}$ is the equivalent shear stress, and $\widetilde{I} = -\mathrm{tr}(\widetilde{\sigma})$, $\widetilde{\sigma_{\mathrm{eq}}} = \sqrt{3\widetilde{j_2}}$, $\widetilde{j_2} = (1/2)\widetilde{S_{ij}}\widetilde{S_{ij}}$, and $\widetilde{j_2} = \det \widetilde{S}$, where $\widetilde{S}$ is the damage deviation stress tensor. The parameter c_1 is the inverse of the slope of the failure surface, and c_2 is related to the ultimate tensile strength of the material.

Generally, the failure surface is considered as the ultimate state of a yield surface. According to the plastic hardening law, the yield surface can be defined as follows:

$$f_p = \widetilde{\sigma_{\mathrm{eq}}} - \alpha_p\left(\gamma_p\right)\widetilde{\sigma_c} = 0, \tag{19}$$

where $\widetilde{\sigma_c} = ((C_2 + \widetilde{I}/f_{c0})/c_1) f_{c0}$. The scalar-valued function $\alpha_p(\gamma_p)$ defines the plastic hardening law of materials, which can be expressed as:

$$\alpha_p\left(\gamma_p\right) = \frac{\gamma_p}{A_3 + \gamma_p}, \tag{20}$$

where $\gamma_p = \int d\gamma_p$, $d\gamma_p = \sqrt{(2/3) de_{ij}^p de_{ij}^p}$, $e_{ij}^p = \varepsilon_{ij}^p - (1/3)\varepsilon_{kk}^p \delta_{ij}$, and the parameter A_3 controls the kinetics of plastic hardening. Note that the failure surface is created when $\alpha_p(\gamma_p) = 1$.

When subjected to compressive stress, the volume of the mortars shrank in the initial stage. According to the generation and propagation of cracks in mortars, there would normally be a transition from compressibility to dilatancy as the applied stress further increased. To describe this transition,

the nonassociated plastic flow rule proposed by Pietruszczak et al. [12] has been used here:

$$g_p = \tilde{\sigma} + \eta_c \bar{I} \ln\left(\frac{\bar{I}}{\bar{I}_0}\right) = 0, \tag{21}$$

where $\bar{I} = c_2 f_{c0} + \tilde{I}$, $\bar{I}_0$ defines the intersection of the plastic potential surface with the $\bar{I}$ axis, and η_c is the slope of the transition line between compressibility and dilatancy.

The plastic constitutive model of concrete can be expressed as follows:

$$d\varepsilon_{ij}^p = d\lambda_p \frac{\partial g_p(\tilde{\sigma}, D)}{\partial \tilde{\sigma}_{ij}}, \tag{22}$$

where $d\lambda_p$ is the plastic factor. When $f_p = 0$, according to the plastic compatibility conditions, $f_p' = 0$. Assuming that damage evolution can be ignored ($d(D) = 0$), $d\lambda_p$ can be expressed as follows:

$$d\lambda_p = \frac{\left(\partial f_p/\partial\tilde{\sigma}\right) : C(D) : d\varepsilon}{\left(\partial f_p/\partial\tilde{\sigma}\right) : C(D) : \left(\partial g_p/\partial\tilde{\sigma}\right) - \left(\partial f_p/\partial\alpha_p\right) : \left(\partial\alpha_p/\partial\gamma_p\right) : h}, \tag{23}$$

where $h = \sqrt{(2/3)(J:(\partial g/\partial\tilde{\sigma}))(J:(\partial g/\partial\tilde{\sigma}))}$, $J = (1/2)(\delta_{ik}\delta_{jl} + \delta_{il}\delta_{jk}) - (1/3)(\delta_{ij}\delta_{kl})$, and $C(D)$ is the effective elastic stiffness tensor.

3.4. Computational Procedure. The iterative method consisting of elastic prediction and plastic correction was chosen for numerical computation in the proposed elastoplastic damage model. In the numerical computation process, the total damage (D) to materials is made up of mechanical damage and chemical damage. The chemical damage variable d_2, which is related simply to the concentration of the sodium sulfate solution and the number of wet-dry cycles, can be calculated as $d_2 = A_2 - A_2 f(c,t)$. The elastic materials parameters (k and μ) before mechanical damage can also be calculated from the chemical damage variable d_2. The mechanical damage is simply related to the total strain, which is known. As an example, the kth computational step can be described as follows.

(1) After the $(k-1)$-st step, the parameters, including the stress $\sigma^{(k-1)}$, the total strain $\varepsilon^{(k-1)}$, the plastic strain $\varepsilon^{p(k-1)}$, the plastic hardening variable $\gamma_p^{(k-1)}$, and the damage variable $D^{(k-1)}$, have been obtained. Then, the strain increment $d\varepsilon^{(k)}$ is input to the kth step.

(2) The total strain is calculated as $\varepsilon^{(k)} = \varepsilon^{(k-1)} + d\varepsilon^{(k)}$. Based on the proposed damage criterion, the mechanical damage variables $d_1^{(k)}$ are computed, and the total damage is obtained using $D^{(k)} = d_1^{(k)} + d_2$.

(3) Based on the assumption that the strain increment is fully elastic, the stress increment and the total stress are calculated as $d\sigma^{(k)} = C(d_1^{(k)}) : d\varepsilon^{(k)}$ and $\sigma^{(k)} = \sigma^{(k-1)} + d\sigma^{(k)}$ respectively.

Table 1: Initial values of model parameters.

ν	0.19
E_0	17.1 GPa
f_{c0}	48.7 MPa
A_1	1×10^{-4}
A_2	0.45
A_3	0.35
B	1.12×10^{-5}
η_c	0.95
ξ_d^0	2500 Pa
c_1	3.0
c_2	0.15

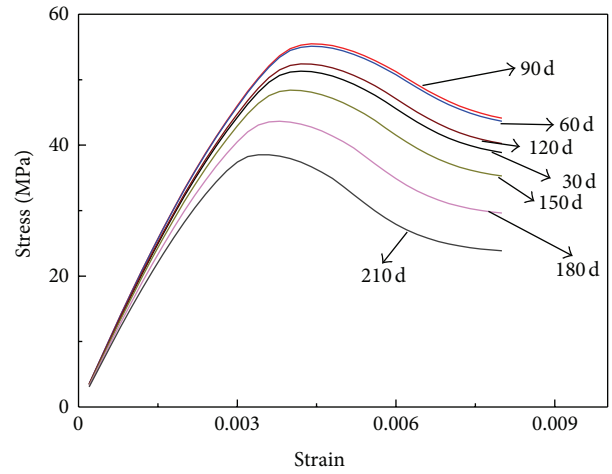

Figure 3: Simulated compressive strength of mortars in 5% sulfate solution after various numbers of wet-dry cycles.

(4) The function $f_p(\sigma^{(k)}, \gamma_p^{(k-1)})$ is used to evaluate whether plastic yielding has occurred.

If $f_p(\sigma^{(k)}, \gamma_p^{(k-1)}) > 0$, plastic yielding has occurred, and the plastic correction must be carried out. An iterative calculation is used to determine the corresponding plastic strain increment $d\varepsilon^{p(k)}$. Then, the increment of the plastic hardening parameter, $d\gamma_p$, is also calculated.

If the function is less than zero, the plastic yielding has not occurred. Update the corresponding variables, and go to the $(k+1)$th step.

4. Numerical Simulations

Using sample subjected to different sulfate solution concentrations and numbers of wet-dry cycles, the parameters involved in the constitutive model were determined by compression tests; the results are presented in Table 1.

Figure 3 presents the simulated compressive strength of mortars in 5% sulfate solution based on the proposed elastoplastic damage model. As the results show, similary to the test data presented in Figure 1(b), the simulated ultimate compressive strength and elastic modulus increased with

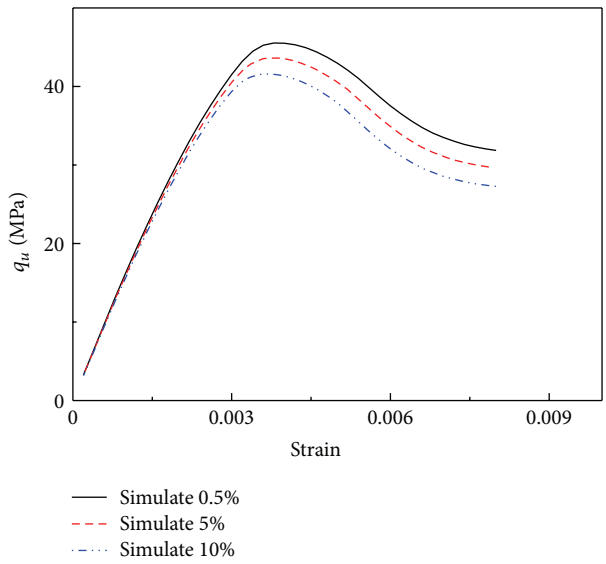

Figure 4: Simulated compressive strength of mortars exposed to various sulfate solution concentrations after 180 wet-dry cycles.

the number of wet-dry cycles in the initial stage. Then, these values began to decrease as the number of wet-dry cycles further increased. Similarly, in axial compressive experiments on concrete specimens, Liu et al. [5] reported that sulfate attack led to decreases in elastic modulus and peak strain. On the other hand, as shown by the simulated results presented in Figure 4, the concentration of the sodium sulfate solution appears to have a significant effect on the mechanical properties of mortars, which is consistent with the test results. Moreover, as shown in Figure 5, the simulated results fit well with the stress-strain curve of the measured values.

Figure 6 presents a comparison between the simulated ultimate compressive strength values and test data for different sulfate solution concentrations and numbers of wet-dry cycles. As the results show, the proposed elastoplastic damage model fitted the test data very well. This indicates that the model is suitable for simulating the mechanical properties of sulfate-attacked mortar subjected to compressive stress.

5. Conclusions

In this study, the mechanical properties of cement mortar in a wet-dry cyclic sulfate attack environment have been investigated. The results showed that the ultimate compressive strength of mortars increased with the number of wet-dry cycles in the early stage. Then, the ultimate strength began to decrease with further increases in the number of wet-dry cycles. In addition, the transition to ultimate strength occurred earlier for samples exposed to higher sulfate solution concentrations.

An elastoplastic damage model was proposed to simulate the mechanical behavior of sulfate-attacked cement mortar subjected to compression stress. The results showed generally good agreement between the simulated values and test data.

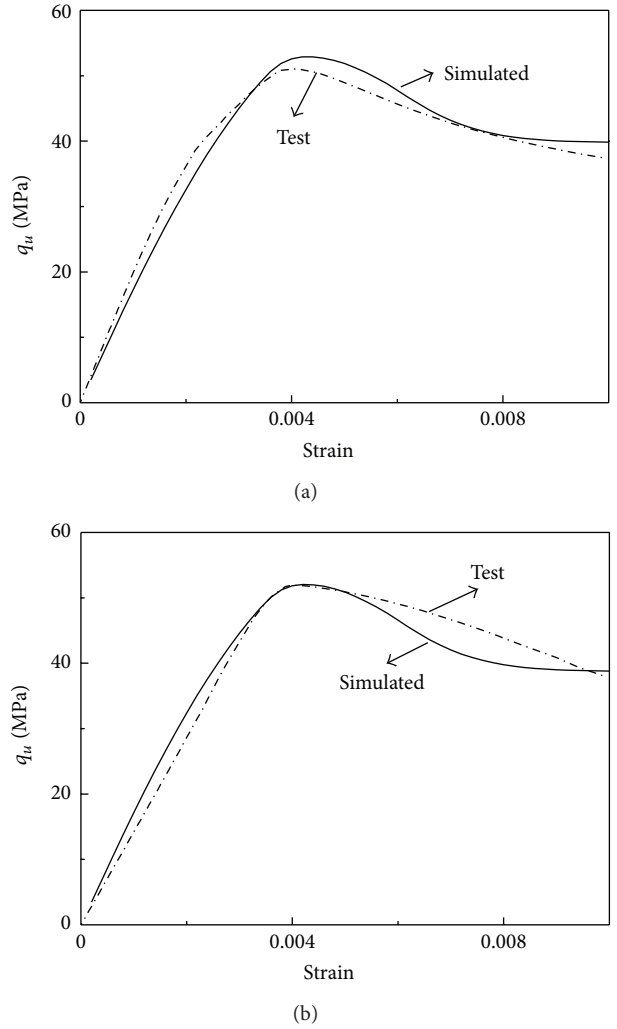

Figure 5: Comparison between simulated compressive strength values and test data for mortars exposed to different sulfate solution concentrations and numbers of wet-dry cycles: (a) mortars in 0.5% sulfate solution after 30 wet-dry cycles; (b) mortars in 10% sulfate solution after 120 wet-dry cycles.

Besides accurately simulating the effects of sulfate concentration and numbers of wet-dry cycles, the proposed model could also capture the main features of observed mechanical behavior. The mechanical behavior of cementitious materials is closely related to the composition of the materials, the water-cement ratio, and other factors. To apply the proposed constitutive model in an engineering environment, the model parameters must be determined from compressive experiments. Once the corresponding parameters have been brought into the constitutive model, the damage progression of the mechanical properties of concrete exposed to a certain sulfate concentration can also be evaluated.

Acknowledgments

The authors are grateful to the National Natural Science Foundation of China (Grant no. 51009061) and the Key

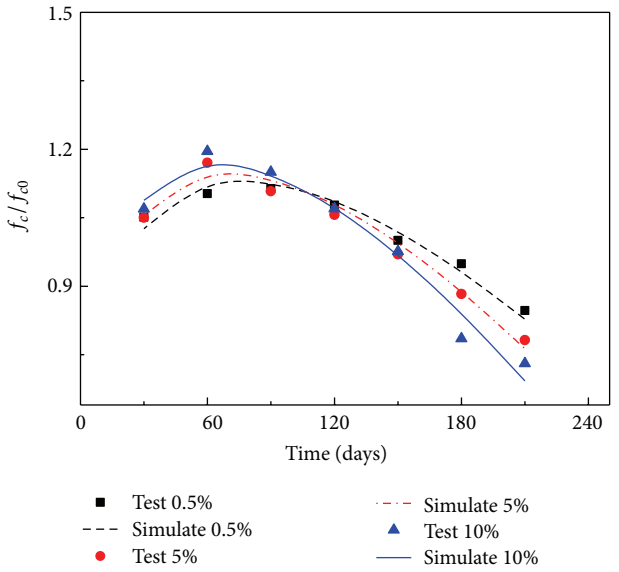

FIGURE 6: Comparison between tested and computed ultimate compressive strength for mortars experiencing different numbers of wet-dry cycles.

Project of the National Natural Science Foundation of Jiangsu Province (BK2011026) for their support of this work.

References

[1] C. Ahmet and Y. Sükrü, "Investigation of mechanical and mineralogical properties of mortars subjected to sulfate," *Construction and Building Materials*, vol. 24, no. 11, pp. 2231–2242, 2010.

[2] R. D. Hooton, "Influence of silica fume replacement of cement on physical properties and resistance to sulfate attack, freezing and thawing, and alkali-silica reactivity," *ACI Materials Journal*, vol. 90, no. 2, pp. 143–151, 1993.

[3] E. F. Irassar, V. L. Bonavetti, and M. González, "Microstructural study of sulfate attack on ordinary and limestone Portland cements at ambient temperature," *Cement and Concrete Research*, vol. 33, no. 1, pp. 31–41, 2003.

[4] S. T. Lee, H. Y. Moon, and R. N. Swamy, "Sulfate attack and role of silica fume in resisting strength loss," *Cement and Concrete Composites*, vol. 27, no. 1, pp. 65–76, 2005.

[5] T. J. Liu, D. J. Zou, J. Teng, and G. L. Yan, "The influence of sulfate attack on the dynamic properties of concrete column," *Construction and Building Materials*, vol. 28, no. 1, pp. 201–207, 2012.

[6] S. Sarkar, S. Mahadevan, J. C. L. Meeussen, H. van der Sloot, and D. S. Kosson, "Numerical simulation of cementitious materials degradation under external sulfate attack," *Cement and Concrete Composites*, vol. 32, no. 3, pp. 241–252, 2010.

[7] A. E. Idiart, C. M. López, and I. Carol, "Chemo-mechanical analysis of concrete cracking and degradation due to external sulfate attack: a meso-scale model," *Cement and Concrete Composites*, vol. 33, no. 3, pp. 411–423, 2011.

[8] J. Lemaitre, *A Course on Damage Mechanics*, Springer, Berlin, Germany, 2nd edition, 1992.

[9] D. Chen, I. Yurtdas, N. Burlion, and J. F. Shao, "Elastoplastic damage behavior of a mortar subjected to compression and desiccation," *Journal of Engineering Mechanics*, vol. 133, no. 4, pp. 464–472, 2007.

[10] H. Xu, *Research on damage behaviour of concrete under sulfate corrosion [Doctoral thesis]*, China University of Mining and Technology, 2012.

[11] D. Sfer, I. Carol, R. Gettu, and G. Etse, "Study of the behavior of concrete under triaxial compression," *Journal of Engineering Mechanics*, vol. 128, no. 2, pp. 156–163, 2002.

[12] S. Pietruszczak, J. Jiang, and F. A. Mirza, "An elastoplastic constitutive model for concrete," *International Journal of Solids and Structures*, vol. 24, no. 7, pp. 705–722, 1988.